ChemistryEurope
Excellence in Chemistry Research Worldwide

Research Article
doi.org/10.1002/ceur.202500296

www.journal.chemistry-europe.org

# Copper-Catalyzed Defluorinative Allylboration of Allenes with Trifluoromethyl Alkenes

Martín Piñeiro-Suárez, Hugo Jiménez-Cristóbal, Israel Fernández,* and Martín Fañanás-Mastral*

An *N*-heterocyclic carbene/Cu-catalyzed coupling of allenes, bis(pinacolato)diboron, and trifluoromethyl alkenes is reported. The method allows access to stereodefined borylated 1,1-difluoro-1,5-dienes with high levels of selectivity. The integration of a 1,5-diene scaffold with boron and fluorine functionalities makes these products versatile building blocks for the synthesis of structurally diverse and valuable organofluorine compounds such as gem-difluoroalkenes, difluoromethylene units, and alkenyl fluorides. Mechanistic studies and density functional theory calculations shed light on key mechanistic aspects of the catalytic process and suggest that the in situ generated LiCl is essential for the reaction by assisting the oxidative addition of the trifluoromethyl alkene to the catalytically generated allylcopper species. It is found that the polarization of the key C—F bond induced upon binding to LiCl results in a significant decrease of destabilizing Pauli repulsion, which is translated into a remarkable reduction of the activation barrier of the oxidative addition step.

## 1. Introduction

Organofluorine compounds are central to modern drug discovery and agrochemical development, given the productive influence that the introduction of specific fluorine motifs in a molecule can have on relevant properties such as conformation, $pK_a$, lipophilicity, metabolic stability, intrinsic potency, and membrane permeability.[1–5] In this context, gem-difluoroalkenes,[6,7] difluoromethylene units,[8] and alkenyl fluorides[9–11] are of particular interest, being important metabolically stable bioisosteres of functional groups such as ketones, alcohols, thiols, or amides (**Scheme 1**a). Not surprisingly, the development of methods for the synthesis of each of these fluorinated motifs has received significant attention in recent years.[12–37] However, general synthetic strategies that enable access to these three organofluorine frameworks from common and readily available starting materials remain notably underdeveloped.

Realizing the synthetic potential of a 1,5-diene structure incorporating both fluorine and boron functionalities, we envisaged that a three-component reaction between an allene, bis(pinacolato)diboron ($B_2pin_2$), and a trifluoromethyl alkene may offer an efficient pathway to a stereodefined, versatile building block that could be easily transformed into a range of fluorinated structures. The 1,5-diene core of the envisioned products may allow the conversion of the gem-difluoroalkene motif into a difluoromethylene unit by thermal Cope rearrangement.[38] Moreover, the presence of the alkenyl boronate provides an extremely useful handle that, besides C—B to C—C bond conversion, may be easily transformed by oxidation into a $\beta,\beta$-difluoroketone prone to undergo E1cB elimination that would lead to an alkenyl fluoride. The proposed three-component reaction would involve the catalytic formation of a borylated allylcopper intermediate that should be capable of reacting with the trifluoromethyl alkene, thus resulting in a net defluorinative allylboration reaction.

Copper-catalyzed allylboration of allenes[39–44] has been previously reported with other allylic electrophiles such as allylic phosphates[45,46] and allylic gem-dichlorides (Scheme 1b).[47] In these transformations, the allyl copper intermediate reacts through the $\alpha$-carbon with the allylic substrate via an $S2'$-oxidative addition followed by reductive elimination to afford the $\alpha,\gamma'$-coupling product with excellent regio- and stereoselectivity.[48] However, the yet elusive[49–52] allylboration of allenes with trifluoromethylalkenes imposes important questions regarding the challenging C—F bond cleavage: 1) The reaction between Cu—B/Cu—Si,[53–56] Cu—H[57] or even Cu—C[58] species with trifluoromethyl alkenes has been

*M. Piñeiro-Suárez, H. Jiménez-Cristóbal, M. Fañanás-Mastral*
*Centro Singular de Investigación en Química Biolóxica e Materiais Moleculares (CiQUS)*
*Departamento de Química Orgánica*
*Universidade de Santiago de Compostela*
*15782 Santiago de Compostela, Spain*
*E-mail: martin.fananas@usc.es*

*I. Fernández*
*Departamento de Química Orgánica and Centro de Innovación en Química Avanzada (ORFEO-CINQA)*
*Facultad de Ciencias Químicas*
*Universidad Complutense de Madrid*
*28040 Madrid, Spain*
*E-mail: israel@quim.ucm.es*

*M. Fañanás-Mastral*
*Oportunius*
*Galician Innovation Agency (GAIN)*
*15702 Santiago de Compostela, Spain*

*Supporting information for this article is available on the WWW under https://doi.org/10.1002/ceur.202500296*

Research Article
doi.org/10.1002/ceur.202500296



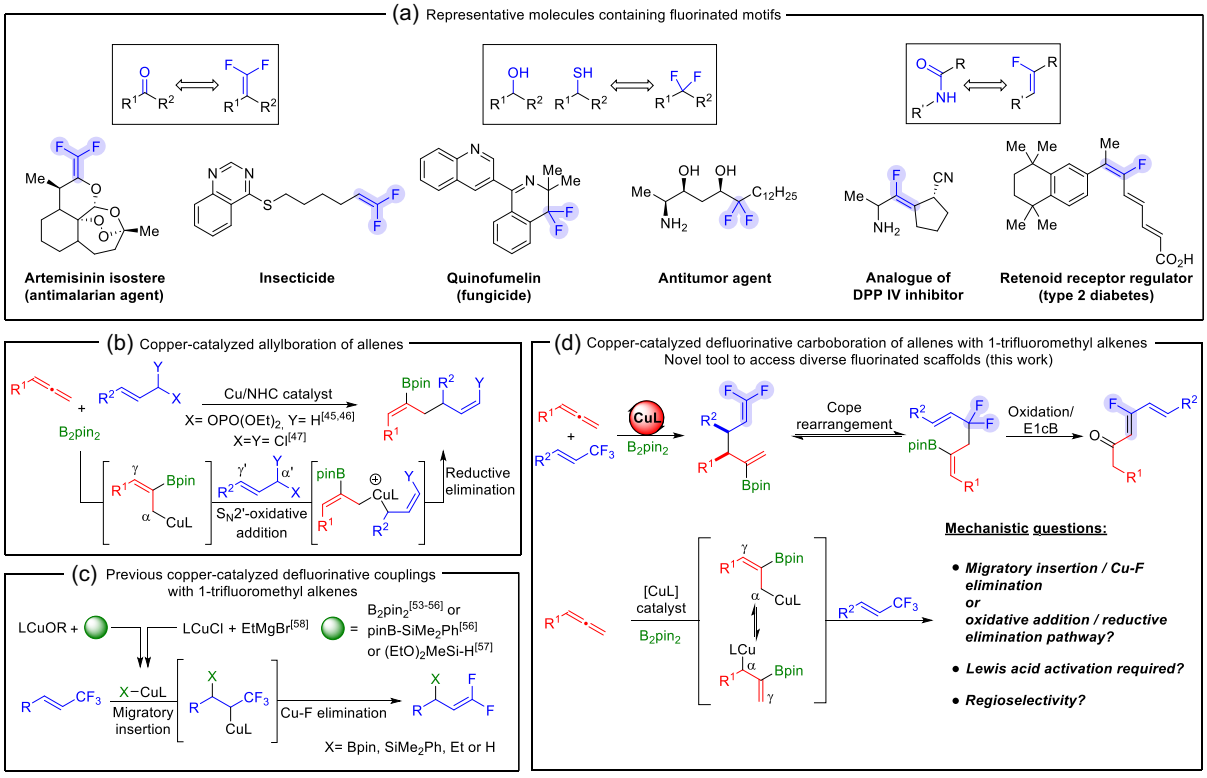


**Scheme 1.** a) Bioisosterism and examples of bioactive compounds featuring *gem*-difluoroalkene, difluoromethylene unit, and alkenyl fluorides. b) Copper-catalyzed allylboration of allenes. c) Previous copper-catalyzed defluorinative couplings with 1-trifluoromethyl alkenes. d) Cu-catalyzed defluorinative allylboration of allenes with 1-trifluoromethyl alkenes (this work)

proposed to occur through an olefin insertion pathway followed by Cu—F elimination (Scheme 1c). Does the process with an allylcopper intermediate evolves in the same way? 2) Is otherwise a pathway involving oxidative addition preferred as reported for copper-catalyzed allylboration of allenes with other more reactive allylic electrophiles?[46,47] 3) Is there any Lewis acid activation required to activate the C—F bond? 4) Finally, regioselectivity may result in an additional challenge since allene borylcupration can lead to the formation of two isomeric allylcopper species that can couple with the trifluoromethyl alkene through either the $\alpha$- or $\gamma$-position.

Herein, we report a copper-catalyzed defluorinative allylboration of allenes that provides borylated difluoro-1,5-dienes with good to excellent levels of chemo-, regio-, and diastereoselectivity (Scheme 1d). The synthetic utility of this new type of borylated difluoro-1,5-dienes is demonstrated with the synthesis of diverse organofluorine structures. In addition, we describe mechanistic studies that have shed light on the above-mentioned questions, unveiling the mode of C—F bond cleavage and the key role of the in situ formed Lewis acid.

## 2. Results and Discussion

### 2.1. Reaction Optimization

We began our study by surveying the reaction between penta-3,4-dien-1-ylbenzene (**1**), (*E*)-1-methyl-4-(3,3,3-trifluoroprop-1-en-1-yl)benzene (**2**), and $B_2pin_2$ (**Table 1**). Initial experiments using IMesCuCl as a catalyst in toluene already showed the challenging nature of this transformation in view of the observed significant lack of reactivity. No reaction took place either when NaO$^t$Bu or KO$^t$Bu was used as a base at 60 °C (entries 1 and 2). The use of LiO$^t$Bu provided the desired product **3** as a 4:1 mixture of *syn*:*anti* diastereomers, albeit the reaction yield was far from satisfactory (entry 3). Interestingly, a similar result was observed when the reaction was carried out with NaO$^t$Bu in the presence of LiCl as an additive (entry 4). Conversely, the use of other Li salts (entries 5 and 6) or other Lewis acids such as trimethylsilyl chloride (TMSCl) (entry 7) as additives was not productive. These results suggested a key role of LiCl, which is catalytically generated when LiO$^t$Bu is used as a base. Screening of other solvents did not produce any further improvement (entries 8 and 9). In contrast, when the reaction was carried out in toluene under more concentrated conditions (0.2 M), product **3** was obtained in a significantly increased yield (entry 10). Evaluation of other ligands revealed that phosphines are not efficient for this transformation (see Supporting Information).

Similarly, *N*-heterocyclic carbene (NHC) ligands bearing *N*-alkyl groups or electron-rich aromatic rings did not yield product **3** (entries 11 and 12). Reactivity was restored by using a saturated imidazolinylidene SIMes ligand (entry 13), although it compares slightly unfavorably with its unsaturated counterpart IMes. Finally, the copper complex derived from the benzimidazolylidene ligand **L2** proved to be the most efficient catalyst for this transformation, furnishing product **3** in 70% yield (entry 14).

Research Article
doi.org/10.1002/ceur.202500296

**Table 1.** Optimization studies.

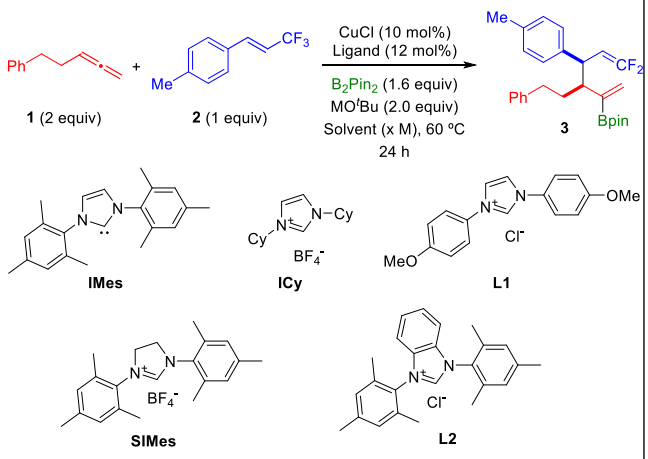


| Entry[a] | M | Additive (2 equiv) | Solvent | Conc.[M] | Ligand | Yield [%][b,c] |
|---|---|---|---|---|---|---|
| 1 | Na | – | Toluene | 0.1 | IMes[d] | – |
| 2 | K | – | Toluene | 0.1 | IMes[d] | – |
| 3 | Li | – | Toluene | 0.1 | IMes[d] | 27 |
| 4 | Na | LiCl | Toluene | 0.1 | IMes[d] | 34 |
| 5 | Na | LiBr | Toluene | 0.1 | IMes[d] | – |
| 6 | Na | LiOTf | Toluene | 0.1 | IMes[d] | 6 |
| 7 | Na | TMSCl | Toluene | 0.1 | IMes[d] | – |
| 8 | Li | – | Dioxane | 0.1 | IMes[d] | – |
| 9 | Li | – | THF | 0.1 | IMes[d] | 24 |
| 10 | Li | – | Toluene | 0.2 | IMes[d] | 63 (55) |
| 11 | Li | – | Toluene | 0.2 | ICy[e] | – |
| 12 | Li | – | Toluene | 0.2 | **L1**[e] | – |
| 13 | Li | – | Toluene | 0.2 | SIMes[e] | 51 |
| 14 | Li | – | Toluene | 0.2 | **L2**[e] | 81 (70) |

[a]Reactions performed on a 0.2 mmol scale. Product **3** was obtained as a 4:1 mixture of *syn*:*anti* diastereomers (structure of the major diastereomer shown). [b]Determined by $^{19}$F-NMR analysis using $PhCF_3$ as internal standard. [c]Yield of isolated product shown in brackets. [d]Commercially available IMesCuCl was used. [e]2.24 equiv of Li$O^tBu$ were used.

Unfortunately, all the attempts to render the reaction enantioselective by using chiral NHC ligands either resulted in nonproductive yields or low enantioselectivity (see Supporting Information for details).

## 2.2. Substrate Scope

Having optimized the reaction conditions, we set out to explore the scope of the reaction (**Table 2**). Allenes bearing aliphatic substituents proved to be efficient substrates and reacted with **2** and $B_2pin_2$, affording borylated difluoro-1,5-dienes **4**-**11** in good yields in almost all cases. Common functional groups such as silyl ether (**5**), ether (**6**), ester (**8**), or carbamate (**9**) were well tolerated. Furthermore, the reaction showed a remarkable chemoselectivity for substrates bearing an alkyne (**10**) or a terminal double bond (**11**) with no formation of side products arising from competitive Cu–Bpin alkyne or olefin insertion.

Interestingly, remarkably different reaction outcomes were observed for allenes bearing a Lewis basic ester group in their aliphatic substituent, depending on its relative position to the allene site. While borylated difluoro-1,5-diene **8** could be efficiently synthesized, no product formation was observed in the attempted generation of **7**. In the case of the latter, the Lewis basic carbonyl group may be properly situated to chelate the Cu atom,[46,59] thus resulting in reactivity inhibition (see below for mechanistic implications). Unfortunately, aryl-substituted allenes were not suitable for this transformation (**12**).

Different trifluoromethyl alkenes were also evaluated for this defluorinative carboboration reaction. Substrates bearing a biphenyl group (**13**) or electron-rich aryl rings (**14**, **15**) proved to be very effective and provided the products with total chemo- and regioselectivity. Halogenated aromatic substrates also furnished the corresponding difluoro-1,5-dienes (**16**, **17**), albeit with slightly diminished yield. Sterically demanding units such as *ortho*-substituted aryl rings (**18**) or a naphthalene group (**19**) were also tolerated, although some regioselectivity erosion was observed in those cases, and the corresponding products were obtained together with significant amounts of the linear isomer. Hetereoaromatic substrates could also be used with high selectivity, as demonstrated with the synthesis of thiophene derivative **20** (70% yield, 8:1 dr). In contrast, 3-alkyl (**21**) or 2-substituted (**22**) trifuoromethyl alkenes were not compatible with the three-component reaction since they showed a preferred reactivity toward direct borylation.[53–56]

## 2.3. Synthetic Modifications

As initially envisioned, the products obtained from the Cu-catalyzed defluorinative carboboration of allenes proved to be versatile compounds for the synthesis of a range of different fluorinated structures (**Scheme 2**). Stereospecific synthesis of ketone **23** was possible by C—B bond oxidation of **3**. This borylated difluoro-1,5-diene underwent stereospecific thermal Cope rearrangement to provide allylic difluoride **24** in a 4:1 *Z*,*E*:*E*,*E* ratio that resembles the dr observed in compound **3**. Product distribution analysis reflected an equilibrium between **3** and **24**, which could be easily separated by column chromatography.

Interestingly, control of reaction conditions in the oxidation of **24** allowed to selectively obtain either difluoromethylene ketone **25** by treatment with sodium perborate or dienyl fluoride **26** by reaction with $H_2O_2$ under basic conditions. The latter transformation likely involves the generation of a boron enolate followed by E1cB elimination.[60] Compound **3** also underwent efficient Suzuki coupling to furnish 1,1-difluoro-1,5-diene **27**. Notably, a minimal change in reaction conditions involving a higher temperature allowed **3** to be directly transformed into the rearranged difluoromethylene-bridged 1,5-diene **28**. These transformations clearly illustrate the synthetic versatility of our defluorinative carboboration strategy that opens the opportunity for the divergent synthesis of many fluorinated products with potential interest in medicinal chemistry via C–Bpin transformations.

Research Article
doi.org/10.1002/ceur.202500296



**Table 2.** Scope of the reaction.

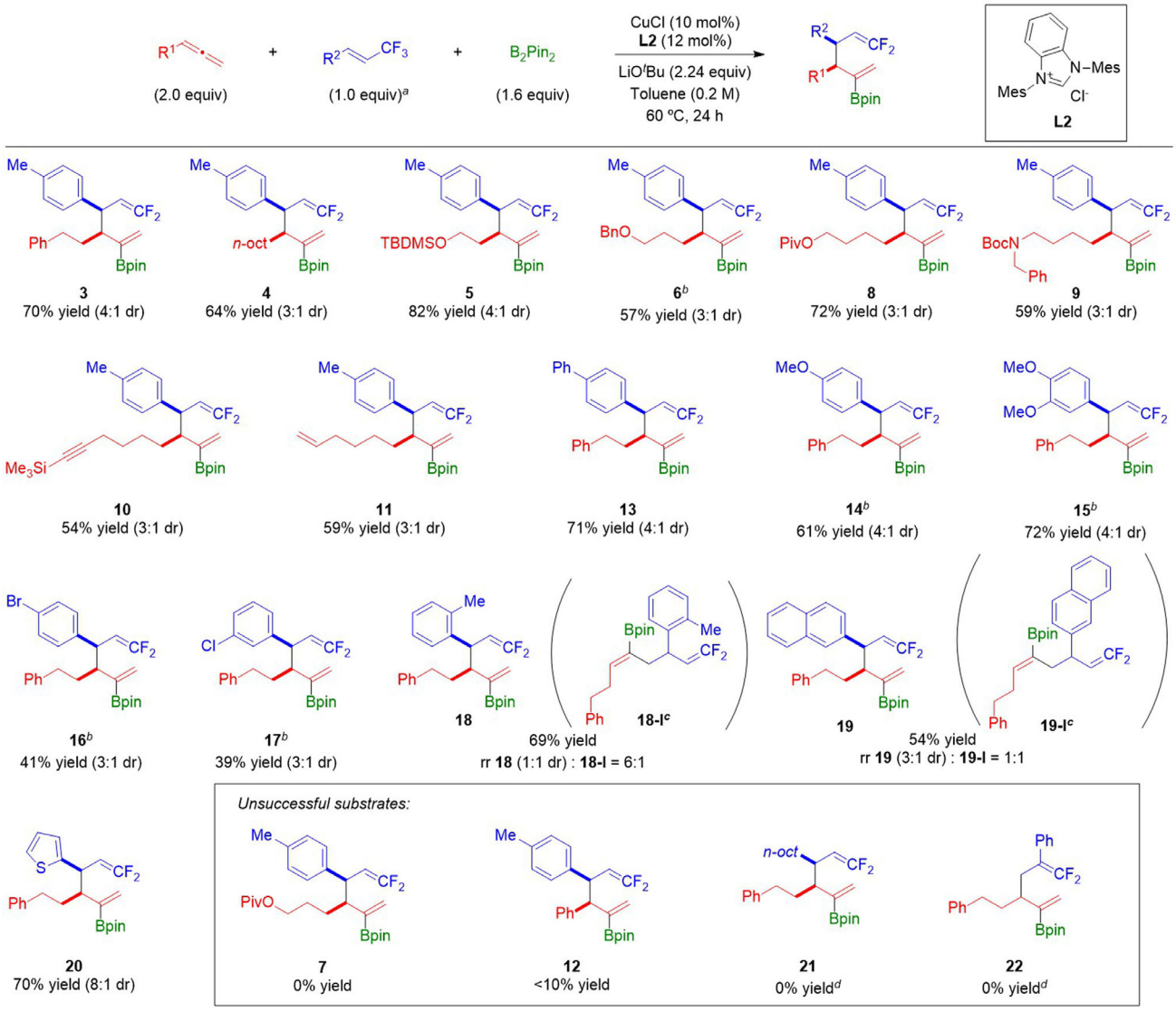


[a]Reactions were performed on a 0.2 mmol scale under optimized conditions (Table 1, entry 13). Yield values refer to isolated products. [b]Reaction run over 48 h. [c]Obtained as pure *Z* isomer. [d]Borylation of trifluoromethyl alkene was observed.

### 2.4. Mechanistic Investigations

As noted above, another main objective of this work was to address several mechanistic questions. Already observed during our optimization studies (Table 1) is the fact that in situ formed LiCl has a profound effect on the reaction outcome, likely suggesting the requirement of Lewis acid activation. The key role of LiCl was further supported by a series of control experiments run using $SIMesBF_4$ as ligand in combination with different copper sources (**Scheme 3**).

While the use of CuCl, which generates LiCl by reaction with LiO$^t$Bu, furnished product **3** in good yield, a dramatic decrease in reactivity was observed when the reaction was carried out with CuI, $[Cu(CH_3CN)_4]BF_4$, and CuOTf, where LiI, $LiBF_4$, and LiOTf are formed, respectively. These results further highlight the key role of the Li cation in enabling efficient defluorinative carboboration, while also indicating the superior performance of LiCl.

Density functional theory (DFT) calculations at the dispersion-corrected polarizable continuum model (PCM)(toluene)-B3LYP-D3/def2-SVP level were performed to gather more insight into the remarkable effect of LiCl and its influence on the key C—F bond-breaking step. **Figure 1** depicts the computed reaction profile using a slightly simplified set of reactants [1,2-pentadiene (**1M**), (3,3,3-trifluoroprop-1-en-1-yl)benzene (**2M**), and $B_2pin_2$] and IMes as ligand.

We first observed that both **INT0**[61] and **INT1** are almost equally affordable upon insertion of **1M** into the Cu(IMes)Bpin complex. Moreover, these species readily undergo isomerization through **TS1**, a saddle point associated with a 1,3-metallotropic rearrangement, with a rather low energy barrier of only

Research Article
doi.org/10.1002/ceur.202500296



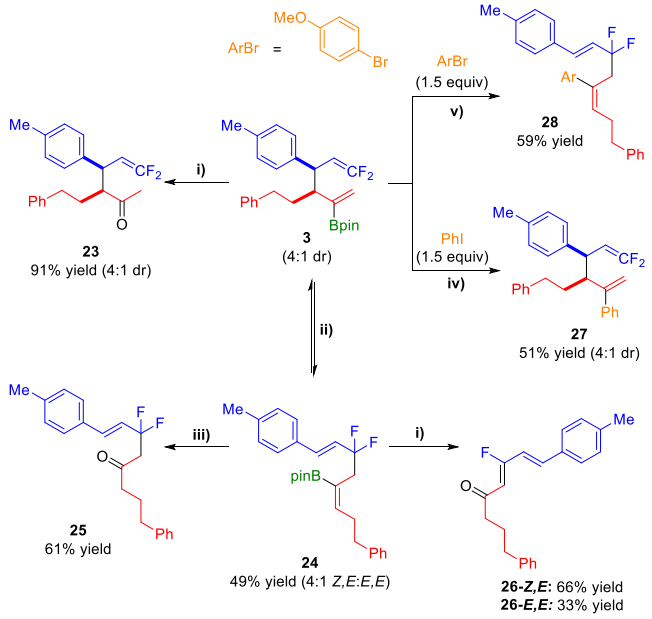


**Scheme 2.** Synthetic modifications of products. Conditions: i) $H_2O_2$, NaOH 2 M, THF, rt, 3 h; ii) Toluene 0.1M, 100 °C, 16 h; iii) $NaBO_3{\cdot}4H_2O$ (5 equiv), THF:$H_2O$, rt, 18 h; iv) $Pd(PPh_3)_4$ (10 mol%), NaOH (2 equiv), Dioxane, 70 °C, 18 h; v) $Pd(PPh_3)_4$ (10 mol%), NaOH (2 equiv), Dioxane, 100 °C, 18 h. Starting from pure *syn*−3.

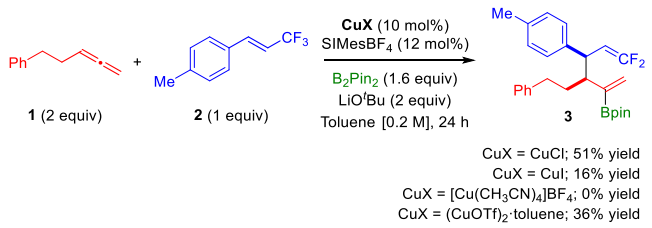


**Scheme 3.** Control experiments using different Cu sources.

6.6 kcal mol$^{-1}$. Coordination of the trifluoromethyl substituted alkene to the transition metal in **INT1** produces **INT2** in a slightly endergonic step ($\Delta G_R = 8.2$ kcal mol$^{-1}$) as a consequence of entropic effects (in fact, the process becomes exothermic, $\Delta H = -10.4$ kcal mol$^{-1}$, when entropy is not considered). From **INT2** two alternative reaction steps can be envisaged according to the literature precedents (see above), namely an insertion reaction via **TS2** (followed by a subsequent Cu—F elimination) or an oxidative addition involving the formation of a Cu—F bond via **TS2'**, which would be followed by a reductive elimination step forming the new C—C bond. From the data shown in Figure 1, it becomes evident that both reactions, and particularly the latter, are not favorable according to the high activation barriers computed for both transformations. Nevertheless, we found that binding of LiCl to one of the fluorine atoms in **INT2** leads to the exergonic formation ($\Delta G_R = -2.4$ kcal mol$^{-1}$) of the related intermediate **INT3'**. From this species, the two alternative pathways similar to those involving **INT2** may take place.

Not surprisingly, the polarization induced by LiCl significantly enhanced the kinetics of both processes, becoming much more favorable. In particular, the oxidative addition pathway via **TS3'** proceeds with a rather low barrier of only 5.5 kcal mol$^{-1}$ and therefore, is preferred over the alternative insertion reaction via **TS3** ($\Delta\Delta G^{\neq} = 11.9$ kcal/mol). This transformation leads to the exergonic formation ($\Delta G_R = -2.6$ kcal mol$^{-1}$) of intermediate **INT4**, which affords the observed product (after releasing the transition metal fragment) through a reductive elimination step via **TS4** (with a barrier of ca. 10 kcal/mol).[62] Moreover, we located two possible transition states associated with the reductive elimination step, **TS4-syn** and **TS4-anti**, which lead to the *syn* and *anti* isomers, respectively. Interestingly, our calculations indicate that the former is more stable than the latter ($\Delta\Delta G^{\neq} = 1.5$ kcal mol$^{-1}$), which is consistent with the preferred formation of the syn-isomer observed experimentally. With the help of the NCIPlot method,[63] we found that the preferred transition state **TS4-syn** is further stabilized by the occurence of CH···$\pi$ interactions involving the ethyl group of the initial allene and the phenyl group of the trifluoromethyl alkene which is absent in its **TS4-anti** counterpart (**Figure 2**). This additional noncovalent interaction is likely responsible for the stereochemical preference observed experimentally.

The key role of LiCl in the transformation deserves further analysis. Therefore, we explored the factors leading to the computed drastic reduction of the activation energy barrier of the preferred oxidative addition step in the presence of LiCl. To this end, we applied the Activation Strain Model (ASM)[64–67] of reactivity to compare the processes involving **TS2'** and the analogous reaction assisted by LiCl involving **TS3'**.

The ASM approach involves decomposing the electronic energy ($\Delta E$) into two terms: the strain energy ($\Delta E_{strain}$) resulting from the distortion of the individual reactants and the interaction ($\Delta E_{int}$) between the deformed reactants along the reaction coordinate, defined in this case by the rupture of the key C…F bond. As these transformations occur intramolecularly, the fragments, i.e., the trifluoromethyl alkene ligand and the allyl–copper complex, need to be referred to the geometry they adopt in the corresponding initial intermediates **INT2** and **INT3'**, constituting therefore the zero level of the different ASM terms. **Figure 3** shows the corresponding activation strain diagrams computed for both oxidative addition reactions from the initial intermediates up to the respective transition states. From the data shown in Figure 3, it becomes clear that the lower barrier computed for the LiCl-assisted reaction results mainly from a stronger interaction between the deformed reactants along the entire reaction coordinate. The contribution of the strain term, which is also less destabilizing for the reaction involving LiCl, is comparatively much less pronounced. For instance, at the same consistent C···F bond-breaking distance of 1.86 Å, the difference in the interaction energy is $\Delta\Delta E_{int} = 18.3$ kcal mol$^{-1}$, whereas a much lower value is observed for the strain term, $\Delta\Delta E_{strain} = 5.1$ kcal mol$^{-1}$, both favoring the LiCl-assisted transformation.

Reasons for the stronger interaction between the trifluoromethyl alkene ligand and the allyl-copper moiety in the LiCl-assisted reaction can be again initially traced with the help of the NCIPlot method,[63] which indicates that the transition state **TS3'** is clearly stabilized by the presence of a $Li^+$···$\pi$ interaction

ChemistryEurope
Excellence in Chemistry Research Worldwide

Research Article
doi.org/10.1002/ceur.202500296

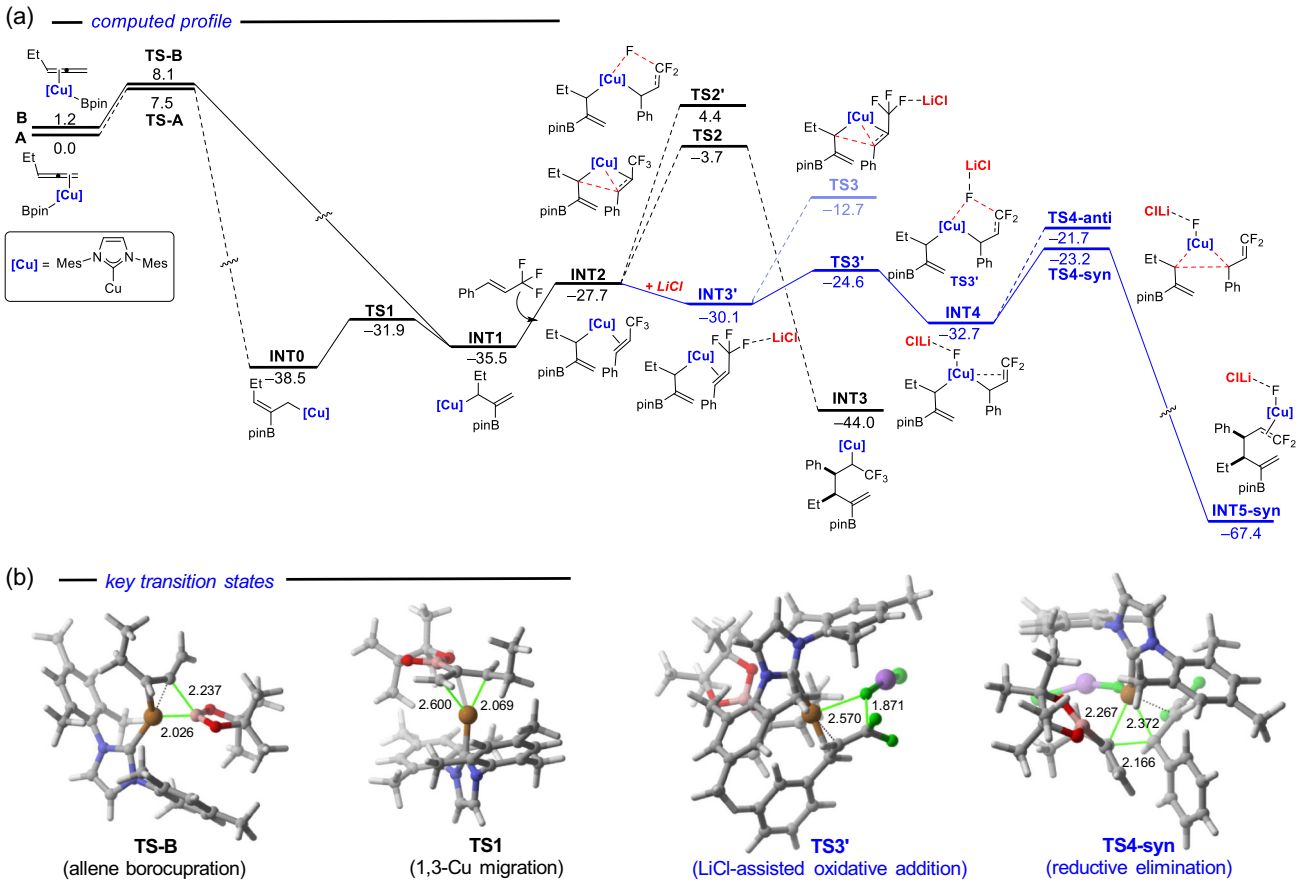


**Figure 1.** a) computed reaction profile for the copper-catalyzed defluorinative allylboration reaction starting from allene complexes **A**/**B**. b) Key transition states in the process. Relative free energies (Δ*G*, at 333.15 K) and bond distances are given in kcal/mol and angstroms, respectively. All data were computed at the PCM(toluene)-B3LYP-D3/def2-SVP level.

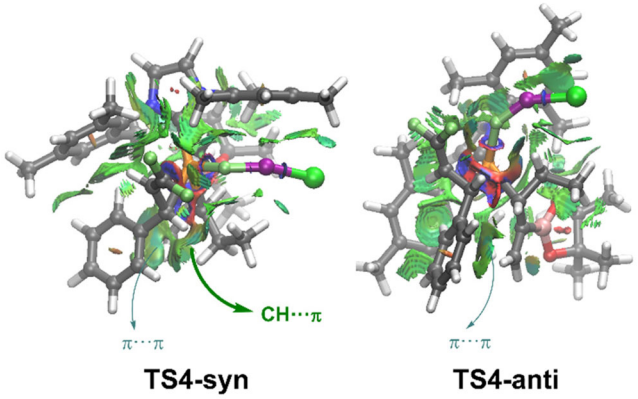


**Figure 2.** Contour plots of the reduced density gradient isosurfaces (density cutoff of 0.04 a.u.) for **TS4-syn** and **TS4-anti.**

established between the lithium atom and one of the mesityl groups of the NHC ligand attached to the transition metal (**Figure 4**). Obviously, this stabilizing interaction, which persists along the entire reaction coordinate (see Figure 2), is absent in the analogous, nonassisted, transition state **TS2′**.

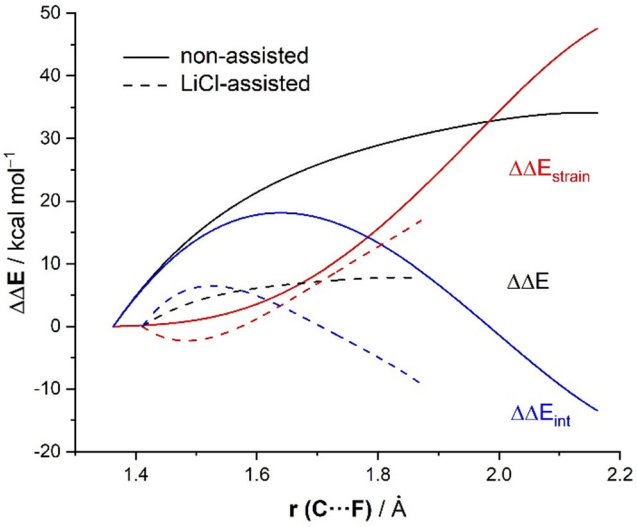


**Figure 3.** Comparative activation strain analyses of the key oxidative addition reaction in the absence (solid lines) or presence (dashed lines) of LiCl and projected onto the C···F bond-breaking distance. All data have been computed at the ZORA-B3LYP-D3/DZP//PCM(toluene)-B3LYP-D3/def2-SVP level.

Research Article
doi.org/10.1002/ceur.202500296



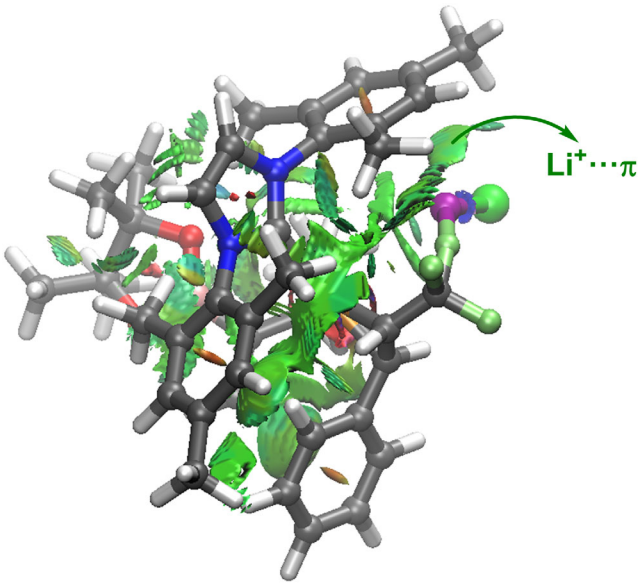


**Figure 4.** Contour plots of the reduced density gradient isosurfaces (density cutoff of 0.04 a.u.) for **TS3'**.

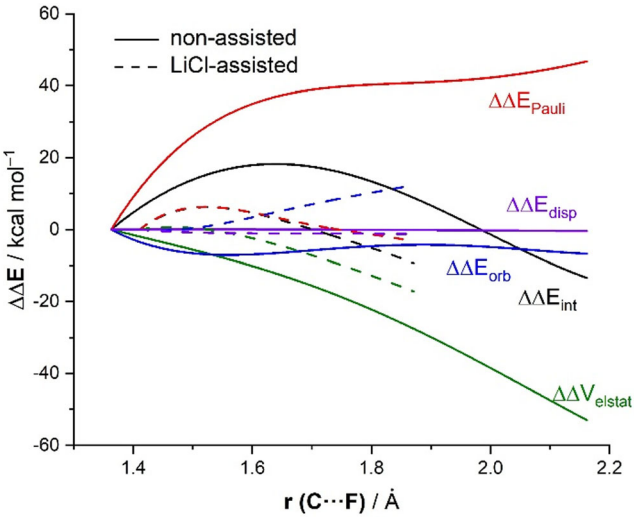


**Figure 5.** EDA of the key oxidative addition reaction in the absence (solid lines) or presence (dashed lines) of LiCl and projected onto the C···F bond-breaking distance. All data have been computed at the ZORA-B3LYP-D3/DZP//PCM(toluene)-B3LYP-D3/def2-SVP level.

Although the occurrence of the above-mentioned $Li^{+}\cdots\pi$ noncovalent interaction certainly contributes to the stabilization of **TS3'**, more quantitative insight into the stronger interaction computed for the LiCl-assisted oxidative addition can be gained by applying the Energy Decomposition Analysis (EDA) method.[68–71] This approach involves decomposing the $\Delta E_{int}$ into the following chemically meaningful terms: classical electrostatic interaction ($\Delta V_{elstat}$), Pauli repulsion ($\Delta E_{Pauli}$) between closed-shell orbitals, which is responsible for steric repulsion, stabilizing orbital attractions ($\Delta E_{orb}$), and interactions coming from dispersion interactions ($\Delta E_{disp}$). As graphically depicted in **Figure 5**, which shows the evolution of the EDA terms along the reaction coordinate and referred again to the starting intermediates, it becomes clear that the much lower barrier computed for the LiCl-assisted process primarily originates from a much less destabilizing Pauli repulsion along the entire reaction coordinate. This is the result of the significant polarization induced by LiCl on the C—F bond, which efficiently depopulates the migrating fluorine atom (as confirmed by the computed natural charge of −0.68 vs −0.73 e, in **TS3'** and **TS2'**, respectively). Consequently, the destabilizing four-electron repulsion between the doubly occupied d atomic orbital of the transition metal and the $\sigma$(C—F) molecular orbital of the alkene ligand becomes much lower, which is translated into the computed lower $\Delta\Delta E_{Pauli}$.[72]

## 3. Conclusion

In summary, we have disclosed a catalytic borylative defluorinative coupling between allenes and trifluoromethyl alkenes. The unprecedented use of this type of fluorinated electrophiles for an unsaturated hydrocarbon allylboration reaction provides stereodefined borylated 1,1-difluoro-1,5-dienes, which serve as highly versatile building blocks for the synthesis of structurally diverse fluorinated compounds that contain medicinally relevant motifs such as gem-difluoroalkenes, difluoromethylene units, and alkenyl fluorides. Intrinsic features of the mechanism could be unveiled with the help of DFT calculations, showcasing the crucial role of catalytically generated LiCl in significantly reducing the activation barrier of the key oxidative addition step.

## *Supporting Information*

List of starting materials, optimization studies, experimental procedures, compound characterization data, NMR spectra, computational methods, cartesian coordinates and electronic energies of all the stationary points discussed. The authors have cited additional references within the Supporting Information.[73–108]

## *Acknowledgements*

Financial support from the MICIU/AEI (Grant nos. PID2020-118237RB-I00, PID2022-139318NB-I00, and RED2022-134331-T), European Research Council (grant no. 863914), Xunta de Galicia (grant no. ED431C 2022/27; Centro de investigación do Sistema universitario de Galicia accreditation (grant nos. 2023−2027, ED431G 2023/03), and the European Regional Development Fund (ERDF) is gratefully acknowledged. M.P.S. and H.J.C. thank Agencia Estatal de Investigación (AEI) for predoctoral fellowships PRE2021−097283 and FPU23/01772, respectively.

## *Conflicts of Interest*

The authors declares no conflicts of interest.

## *Data Availability Statement*

The data that support the findings of this study are available in the supplementary material of this article.

Research Article
doi.org/10.1002/ceur.202500296



**Keywords:** activation strain model-energy decomposition analysis · carboboration · copper · organofluorine compounds · pauli repulsion

[1] K. Müller, C. Faeh, F. Diederich, *Science* **2007**, *317*, 1881.
[2] S. Purser, P. R. Moore, S. Swallow, V. Gouverneur, *Chem. Soc. Rev.* **2008**, *37*, 320.
[3] T. Fujiwara, D. O'Hagan, *J. Fluorine Chem.* **2014**, *167*, 16.
[4] E. P. Gillis, K. J. Eastman, M. D. Hill, D. J. Donnelly, N. A. Meanwell, *J. Med. Chem.* **2015**, *58*, 8315.
[5] T. Liang, C. N. Neumann, T. Ritter, *Angew. Chem. Int. Ed.* **2013**, *52*, 8214.
[6] C. Leriche, X. He, C. T. Chang, H. Liu, *J. Am. Chem. Soc.* **2003**, *125*, 6348.
[7] G. Magueur, B. Crousse, M. Ourévitch, D. Bonnet-Delpon, J.-P. Bégué, *J. Fluorine Chem.* **2006**, *127*, 637.
[8] N. A. Meanwell, *J. Med. Chem.* **2011**, *54*, 2529.
[9] B. Malo-Forest, G. Landelle, J.-A. Roy, J. Lacroix, R. C. Gaudreault, J.-F. Paquin, *Bioorg. Med. Chem. Lett.* **2013**, *23*, 1712.
[10] Y. Asahina, K. Iwase, F. Iinuma, M. Hosaka, T. Ishizaki, *J. Med. Chem.* **2005**, *48*, 3194.
[11] R. A. Altman, K. K. Sharma, L. G. Rajewski, P. C. Toren, M. J. Baltezor, M. Pal, S. N. Karad, *ACS Chem. Neurosci.* **2018**, *9*, 1735.
[12] For reviews on the synthesis of organofluorine compounds, see refs. 13-17.
[13] T. Fujita, K. Fuchibe, J. Ichikawa, *Angew. Chem. Int. Ed.* **2019**, *58*, 390.
[14] M. Wang, Z. Shi, *Chem. Lett.* **2021**, *50*, 553.
[15] F. Zhao, W. Zhou, Z. Zuo, *Adv. Synth. Catal.* **2022**, *364*, 234.
[16] L. V. Hooker, J. S. Bandar, *Angew. Chem. Int. Ed.* **2023**, *62*, e202308880.
[17] E. M. Eliwa, A. H. Bedair, J.-P. Djukic, *Org. Biomol. Chem.* **2024**, *22*, 6860.
[18] For recent selected examples on the synthesis of gem-difluoroalkenes, see refs 19-23.
[19] J. Tian, L. Zhou, *Chem. Sci.* **2023**, *14*, 6045.
[20] Y. Li, W.-S. Zhang, S.-N. Yang, X.-Y. Wang, Y. Liu, D.-W. Ji, Q.-A. Chen, *Angew. Chem. Int. Ed.* **2023**, *62*, e202300036.
[21] P. Bellotti, H.-M. Huang, T. Faber, R. Laskar, F. Glorius, *Chem. Sci.* **2022**, *13*, 7855.
[22] C. Luo, Y. Zhou, H. Chen, T. Wang, Z.-B. Zhang, P. Han, L.-H. Jing, *Org. Lett.* **2022**, *24*, 4286.
[23] P. Martínez-Balart, Á. Velasco-Rubio, S. Barbeira-Arán, H. Jiménez-Cristóbal, M. Fañanás-Mastral, *Green Chem.* **2024**, *26*, 11196.
[24] For recent selected examples on the synthesis of difluoromethylene units, see refs 25-31.
[25] L. Wen, N. Zhou, Z. Zhang, C. Liu, S. Xu, P. Feng, H. Li, *Org. Lett.* **2023**, *25*, 3308.
[26] Z.-J. Shen, C. Zhu, X. Zhang, C. Yang, M. Rueping, L. Guo, W. Xia, *Angew. Chem. Int. Ed.* **2023**, *62*, e202217244.
[27] A. Messara, A. Panossian, K. Mikami, G. Hanquet, F. R. Leroux, *Angew. Chem. Int. Ed.* **2023**, *62*, e202215899.
[28] S. E. Wright, J. S. Bandar, *J. Am. Chem. Soc.* **2022**, *144*, 13032.
[29] K. Muta, K. Okamoto, H. Nakayama, S. Wada, A. Nagaki, *Nat. Commun.* **2025**, *16*, 416.
[30] Z.-X. Wang, K. Livingstone, C. Hümpel, C. G. Daniliuc, C. Mück-Lichtenfeld, R. Gilmour, *Nat. Chem.* **2023**, *15*, 1515.
[31] M. Chen, Y. Cui, X. Chen, R. Shang, X. Zhang, *Nat. Commun.* **2024**, *15*, 419.
[32] For recent selected examples on the synthesis of alkenyl fluorides see refs 33-37.
[33] D. Zeng, Z. Liu, G. Huang, Y. Wang, S. Zhu, *Nat. Commun.* **2024**, *15*, 7645.
[34] X. Huang, M. Ou, L. Hong, W. Qin, Y. Ma, *ACS Catal.* **2024**, *14*, 6432.
[35] S. Porey, Y. Bairagi, S. Guin, X. Zhang, D. Maiti, *ACS Catal.* **2023**, *13*, 14000.
[36] Y. Wang, G. C. Tsui, *Org. Lett.* **2024**, *26*, 5822.
[37] S. Akiyama, K. Kubota, M. S. Mikus, P. H. S. Paioti, F. Romiti, Q. Liu, Y. Zhou, A. H. Hoveyda, H. Ito, *Angew. Chem. Int. Ed.* **2019**, *58*, 11998.
[38] C. Zhu, M.-M. Sun, K. Chen, H. Liu, C. Feng, *Angew. Chem. Int. Ed.* **2021**, *60*, 20237.
[39] For reviews on copper-catalyzed carboboration of unsaturated hydrocarbons, see refs 40-44.
[40] F. J. T. Talbot, Q. Dherbassy, S. Manna, C. Shi, S. Zhang, G. P. Howell, G. J. P. Perry, D. J. Procter, *Angew. Chem. Int. Ed.* **2020**, *59*, 20278.
[41] A. P. Pulis, K. Yeung, D. J. Procter, *Chem. Sci.* **2017**, *8*, 5240.
[42] A. Whyte, A. Torelli, B. Mirabi, A. Zhang, M. Lautens, *ACS Catal.* **2020**, *10*, 11578.
[43] K. K. Das, S. Manna, S. Panda, *Chem. Commun.* **2021**, *57*, 441.
[44] A. Chaves-Pouso, E. Rivera-Chao, M. Fañanás-Mastral, *ACS Catal.* **2023**, *13*, 12656.
[45] K. Semba, N. Bessho, T. Fujihara, J. Terao, Y. Tsuji, *Angew. Chem. Int. Ed.* **2014**, *53*, 9007.
[46] F. Meng, K. P. McGrath, A. H. Hoveyda, *Nature* **2014**, *513*, 367.
[47] M. Piñeiro-Suárez, A. M. Álvarez-Constantino, M. Fañanás-Mastral, *ACS Catal.* **2023**, *13*, 5578.
[48] G. S. Vázquez-Galiñanes, M. Piñeiro-Suárez, B. L. Tóth, F. Maseras, M. Fañanás-Mastral, *J. Am. Chem. Soc.* **2024**, *146*, 21977.
[49] To the best of our knowledge, only two defluorinative carboborations of unsaturated hydrocarbons have been described. One involves the Cu-catalyzed borylative coupling of styrene with perfluorobenzenes, (see refs. 50-51) and the other, a photocatalytic alkylboration of alkenes (see ref. 52).
[50] F.-P. Wu, X.-W. Gu, H.-Q. Geng, X.-F. Wu, *Chem. Sci.* **2023**, *14*, 2342.
[51] Y. Zhao, B. Fu, S. Wang, Y. Li, X. Yuan, J. Yin, T. Xiong, Q. Zhang, *Org. Lett.* **2023**, *25*, 2492.
[52] Y. Fan, Z. Huang, Y. Lu, S. Zhu, L. Chu, *Angew. Chem. Int. Ed.* **2024**, *63*, e202315974.
[53] R. Corberán, N. W. Mszar, A. H. Hoveyda, *Angew. Chem. Int. Ed.* **2011**, *50*, 7079.
[54] R. Kojima, S. Akiyama, H. Ito, *Angew. Chem. Int. Ed.* **2018**, *57*, 7196.
[55] P. Gao, C. Yuan, Y. Zhao, Z. Shi, *Chem* **2018**, *4*, 2201.
[56] P. H. S. Paioti, J. del Pozo, M. S. Mikus, J. Lee, M. J. Koh, F. Romiti, S. Torker, A. H. Hoveyda, *J. Am. Chem. Soc.* **2019**, *141*, 19917.
[57] T. Takata, K. Hirano, M. Miura, *Org. Lett.* **2019**, *21*, 4284.
[58] M. Wang, X. Pu, Y. Zhao, P. Wang, Z. Li, C. Zhu, Z. Shi, *J. Am. Chem. Soc.* **2018**, *140*, 9061.
[59] Y. Xi, T. W. Butcher, J. Zhang, J. F. Hartwig, *Angew. Chem. Int. Ed.* **2016**, *55*, 776.
[60] P. Ryberg, O. Matsson, *J. Org. Chem.* **2002**, *67*, 811.
[61] A direct pathway from INT0 to the branched product could not be found. Furthermore, the evolution of INT0 to the linear product in the presence of LiCl features an energy barrier of 17.1 kcal/mol (see Supporting Information for details), thus suggesting that isomerization to INT1 is preferred. Nevertheless, in cases where the allene bears a sterically demanding substituent (see e.g. products 18 and 19 in Table **2**), this pathway would become competitive thus explaining the formation of the linear product.
[62] In the presence of LiCl, the reductive elimination becomes the rate-limiting step. Under these conditions, a less electron-rich ligand, such as an unsaturated N-heterocyclic carbene (NHC) compared to its saturated analogue, may facilitate this step more effectively. This hypothesis is further supported by the data presented in Table **1**, where NHCs bearing more electron-donating substituents are not efficient for this transformation.
[63] E. R. Johnson, S. Keinan, P. Mori-Sánchez, J. Contreras-García, A. J. Cohen, W. Yang, *J. Am. Chem. Soc.* **2010**, *132*, 6498.
[64] I. Fernández, F. M. Bickelhaupt, *Chem. Soc. Rev.* **2014**, *43*, 4953.
[65] L. P. Wolters, F. M. Bickelhaupt, *WIREs Comput. Mol. Sci.* **2015**, *5*, 324.
[66] F. M. Bickelhaupt, K. N. Houk, *Angew. Chem. Int. Ed.* **2017**, *56*, 10070.
[67] I. Fernández, in *Discovering the Future of Molecular Sciences*, (Ed: B. Pignataro), Wiley-VCH, Weinheim **2014**, pp.165–187.
[68] For reviews on the EDA method, see refs 69-71.
[69] F. M. Bickelhaupt, E. J. Baerends, in *Reviews in Computational Chemistry*, Vol. *15*,(Eds: K. B. L. Lipkowitz, D. B. Boyd),New York, Wiley-VCH **2000**, pp.1–86.
[70] M. von Hopffgarten, G. Frenking, *WIREs Comput. Mol. Sci.* **2012**, *2*, 43.
[71] I. Fernández, in *Applied Theoretical Organic Chemistry*, (Ed. D. J. Tantillo), World Scientific, New Jersey **2018**, pp. 191–226.
[72] For other catalytic processes where the reduction of the Pauli repulsion between occupied molecular orbitals is also translated into lower activation barriers, see: T. A. Hamlin, F. M. Bickelhaupt, I. Fernández, *Acc. Chem. Res.* **2021**, *54*, 1972.

Manuscript received: August 1, 2025
Revised manuscript received: August 26, 2025
Version of record online: